Pathways and Dynamics of Dissociation of Ionized $(H_2O)_2$

R. N. Barnett and Uzi Landman*

School of Physics, Georgia Institute of Technology, Atlanta, Georgia 30332

Received: September 25, 1995[⊗]

The energetics, geometrical and electronic structure, ionization processes, dynamics, and dissociation pathways of neutral and singly and doubly ionized water dimers are investigated with simulations employing the Born−Oppenheimer local-spin-density functional molecular dynamics (BO-LSD-MD) method. Vertical and adiabatic ionization potentials and dissociation energies and barriers are calculated for various dissociation channels of the singly and doubly ionized dimer. A new bound ground-state, $(H_2O)_2^+$(a), with a hydrazine-like configuration, whose energy is lower by 0.22 eV than that of the disproportionated-ion isomer, $(OH)(H_3O)^+$, is found for the singly charged dimer cation. A state with a similar geometry is found for a bound metastable state of the doubly ionized water dimer, whose dissociation into $2(H_2O^+)$ involves a barrier of ~0.68 eV. The dissociation pathways of the singly ionized dimer depend on the internal energy of the parent neutral and on the excitation energy, with the $OH + H_3O^+$ channel dominating at low energies. Fission of the doubly ionized dimer into the $H_2O^+ + H_2O^+$ and $OH^+ + H_3O^+$ channels can be influenced by the ionization process; direct double ionization of the neutral leads mainly to fission into the first channel, while sequential double ionization can lead to the other.

1. Introduction

Structural, energetic, and dynamical properties of water clusters have been the subject of increasing research activities in recent years, due to the ubiquity of H_2O as one of the most important polar solvents[1,2] as well as the importance of water clusters in atmospheric science.[3−9] Such studies[1−39] provide insights into the nature of hydrogen bonding, proton-transfer processes, solvation phenomena, and fundamental mechanisms underyling ion chemistry of the upper atmosphere.

Charged water species (such as the oxonium ion H_3O^+ and $H_3O_2^+$) occur often as solvated charge carriers in aqueous solutions, condensed phases (ices), and clusters (such as the celebrated $(H_2O)_{21}H^+$ cluster which may be described as $(H_2O)_{20}{\cdot}H_3O^+$, i.e., an oxonium hydrated in a cage of 20 water molecules[24]). They also occur in moist air,[11] in flames,[12] and in the D region of the ionosphere, the troposphere, and stratosphere.[3−10]

In this paper we focus on the properties and dissociation pathways of the smallest neutral and ionized water clusters, $(H_2O)_2$, $(H_2O)_2^+$, and $(H_2O)_2^{2+}$, using electronic structure calculations based on the local spin-density (LSD) functional method (with and without generalized exchange-correlations gradient corrections (GGC)), and in conjunction with molecular dynamics (MD) simulations of ionic motion on the ground-state Born−Oppenheimer (BO) potential energy surface (using the BO-LSD-MD method[35]). Our investigations reveal new aspects pertaining to ionization processes of these systems and the complex nature of their potential energy surfaces, where the equilibrium ground-state structure of the neutral dimer differs significantly from those of the ionized species; in particular we identify a new hydrazine-like optimal ground-state molecular configuration for the ionized dimer $(H_2O)_2^+$.

Moreover, we find that even the smallest doubly-ionized water cluster, $(H_2O)_2^{2+}$, possesses a bound metastable state and determine the barrier (~0.68 eV) for its dissociation into $2(H_2O)^+$. These investigations, along with simulations of the dynamics of the dissociation processes of the doubly ionized dimer, showing that a dominant part (~90%) of the released energy is converted into interfragment translational kinetic energy, suggest that the fission pathways depend on the ionization process (i.e., simultaneous double ionization, versus stepwise, sequential single ionization, leading to different dissociation products) and deepen our understanding of such processes. They also provide the impetus for new experiments, including time-resolved fast spectroscopy. Following a brief description in section 2 of the computation and simulation method, we present our results in section 3 and summarize them in section 4.

2. Method

In calculations of the total energies, structural optimization, and molecular dynamics simulations we have used the BO-LSD-MD method.[35] In these calculations we have used nonlocal norm-conserving pseudopotentials[40] for the valence electrons of the oxygen atoms (s- and p- components, with s-nonlocality) and a local pseudopotential for the hydrogens. Both LSD calculations and ones including generalized gradient corrections (GGC; with the exchange gradient correction of Becke[41] and the correlation gradient correction of Perdew[42]) were performed. In the text we quote results from GGC calculations; a comparison between the results of LSD and GGC calculations is given in the tables.

As discussed in detail elsewhere,[35] in our method no supercells (i.e., periodic replicas of the ionic system) are used, thus allowing studies of charged and multipolar clusters in an accurate and straightforward manner. In dynamical simulations the Hellman−Feynman forces on the ions are evaluated between each MD step, involving iterative solution of the LSD Kohn−Sham equations, thus ensuring that the ionic trajectories are followed on the BO potential energy surface. In the LSD and GGC calculations we used plane-wave cutoffs of 96 and 158 Ry, respectively. A typical time step $\Delta t = 0.3$ fs was used in integration of the ionic equations of motion.

3. Results

(a) Singly Charged Cations. Starting from the neutral water dimer, $(H_2O)_2$, in its optimal ground-state configuration (see

[⊗] Abstract published in *Advance ACS Abstracts,* November 15, 1995.

0022-3654/95/2099-17305$09.00/0

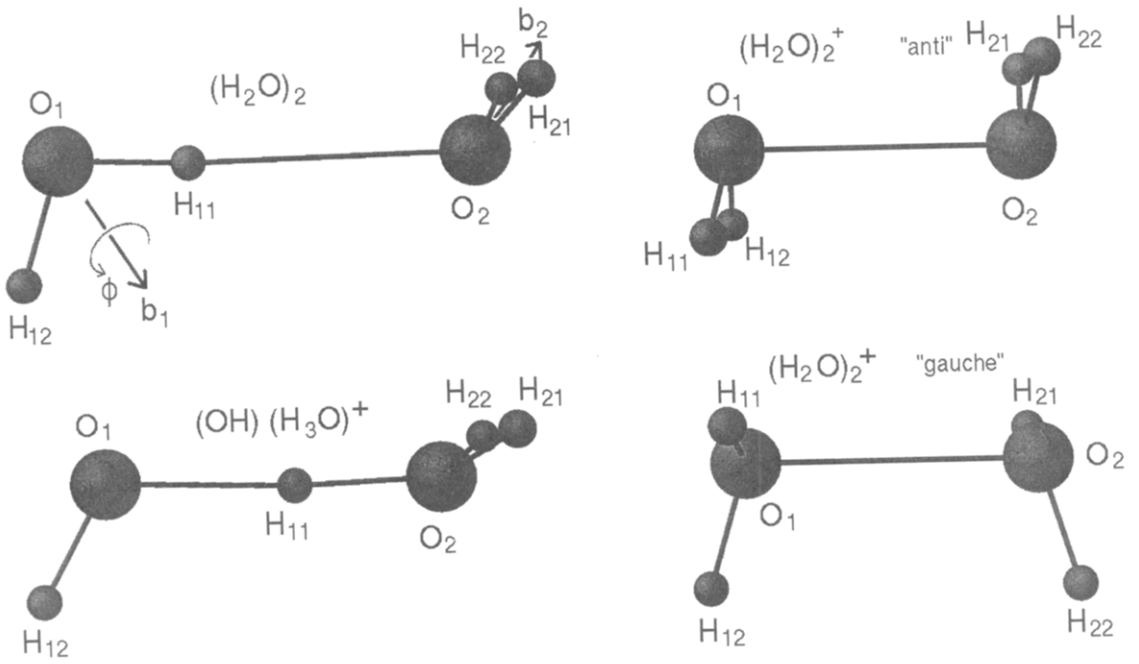

Figure 1. Optimized configurations (calculated at the GGC level) of the ground-state neutral water dimer, $(H_2O)_2$, the hydrazine-like ground-state of the dimer cation ($(H_2O)_2^+$(a), marked "anti") and of the $(H_2O)_2^+$(g) (marked "gauche"), and disproportionated ion, $(OH)(H_3O)^+$, isomers. Large and small spheres denote oxygen and hydrogen atoms, respectively. Geometrical parameters are given in Table 1.

TABLE 1: Geometrical Parameters (Distances in angstroms and Angles in degrees), of the Optimal Structures (Calculated at the GGC Level) for the Neutral Dimer, $(H_2O)_2$, the Singly Charged Dimer Cation in the Disproportionate Ion Configuration, $(OH)(H_2O)^+$, the (a) Ground-State Hydrazine-like Configuration, and the (g) Isomer, and for the (a) and (g) Metastable Bound Isomers of the Doubly Charged Dimer Cation[a]

		$(H_2O)_2^+$			$(H_2O)_2^{2+}$	
	$(H_2O)_2$	$(OH)(H_3O)^+$	(a)	(g)	(a)	(g)
			Distances (Å)			
$H_{11}O_1$	0.976	1.409	0.981	0.980	1.023	1.019
$H_{12}O_1$	0.962	0.987	0.981	0.977	1.023	1.020
$H_{21}O_2$	0.965	0.971	0.981	0.980	1.023	1.019
$H_{22}O_2$	0.965	0.971	0.981	0.977	1.023	1.020
O_1O_2	2.957	2.502	2.176	2.182	1.517	1.491
$H_{11}O_2$	1.982	1.095				
			Angles (deg)			
$\angle(H_{11}O_1H_{12})$	104.2	117.3	104.5	107.9	107.9	114.3
$\angle(B_1O_1O_2)$	125.7	119.7	97.3	105.5	115.4	124.9
ϕ_1	0.0	0.0	90.0	79.8	90.0	85.1
$\angle(H_{21}O_2H_{22})$	104.7	112.5	104.5	107.9	107.9	114.3
$\angle(B_2O_2O_1)$	124.0	144.1	97.3	105.5	115.4	124.9
ϕ_2	90.0	90.0	90.0	79.8	90.0	85.1
$\angle(O_2O_1H_{11})$			94.5	91.1	104.6	104.6
$\angle(O_2O_1H_{12})$			94.5	107.1	104.6	111.6
$\angle(O_1H_{11}O_2)$	177.0	176.0				
			Dihedral Angles (deg)			
$B_1O_1O_2B_2$	180.0	180.0	180.0	104.5	180.0	100.8
$H_{11}O_1O_2H_{22}$			180.0	100.9	180.0	96.5

[a] Points B_1 (or B_2) are on the $\vec{b}_1$ (or $\vec{b}_2$) vector defined as the vector in the corresponding HOH plane, whose origin is on the oxygen (O_1 or O_2), and bisecting the corresponding $\angle$(HOH) angle. ϕ_1 (or ϕ_2) is the angle required in order to rotate the corresponding water molecule (1 or 2) about its $\vec{b}$ vector (defined above), so that the HOH plane of the molecule coincides with the corresponding BO_1O_2 plane.

Figure 1 and Table 1; the calculated binding energy of the neutral is 0.16 eV,[43] compared to 0.23 eV determined experimentally[44]), the vertical ionization potential was calculated to be vIP[$(H_2O)_2$;+] = 11.74 eV (see Figure 2 and Table 2), compared to vIP[H_2O;+] = 12.69 calculated for the H_2O molecule (a measured value[45] of 12.62). The calculated vIP

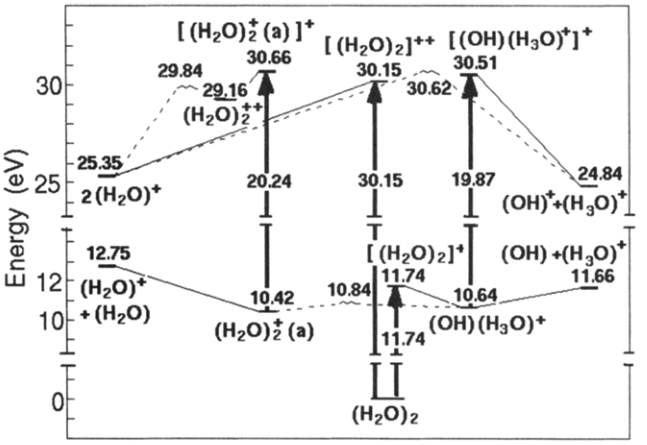

Figure 2. Energy level scheme of various ionized water dimer species, referenced to the energy of the neutral $(H_2O)_2$ molecule. Vertical arrows indicate vertical ionization processes and wiggles denote transition barriers. The horizontal axis denotes a schematic reaction pathway. Square brackets denote a vertically ionized species (i.e., unrelaxed, in the ionic configuration of the parent).

for the dimer is in good agreement with a value of 12.1 ± 0.1 determined from HeI photoelectron measurements.[26] In the $^2A''$ state of the vertically ionized dimer the hole is created on the proton-donor oxygen atom[28,29] (i.e., involving the out-of-plane nonbonding orbital of the proton donor; see Figure 3a). In this context we note that the second vIP (assigned to the $^2A'$ band of the spectrum[26]) was calculated by us to be 13.1 eV, compared to the experimental value[26] of 13.2 ± 0.2 eV, and is due to ionization of an orbital which is a mixture of the in-plane nonbonding orbital of the proton doner and the out-of-plane nonbonding orbital of the proton acceptor (see Figure 3b). Double ionization of $(H_2O)_2$ required an ionization energy vIP-$[(H_2O)_2;++]$ = 30.15 eV (see Figure 2 and Table 2) and the two ionization holes are on the proton-donor and proton-acceptor oxygens of the dimer (see Figure 3c).

The $^2A''$ vertically ionized cation, $[(H_2O)_2]^+$ (in the following square brackets surrounding the molecule denote a vertically ionized state), can undergo a fast (simulated to be about 50 fs)

TABLE 2: Calculated Vertical and Adiabatic Ionization Potentials (*v*IP and *a*IP, Respectively) for the Ground States of H_2O and $(H_2O)_2$, the Ground-State "Anti" Configuration of the Dimer Cation, $(H_2O)_2^+$(a), and the Disproportionated Ion Isomer, $(OH)(H_3O)^+$[a]

	H_2O		$(H_2O)_2$		$(H_2O)_2^+$(a)		$OH(H_3O)^+$	
	LSD	GGC	LSD	GGC	LSD	GGC	LSD	GGC
*v*IP	13.22	12.69	12.00	11.74	20.12	20.24	20.21	19.87
	(12.62)[b]		(12.1 ± 0.1)[c]					
*a*IP	13.10	12.59	(a) 10.62	10.42	(a) 18.35	18.74	(a) 17.97	18.51
	(12.6)[d]		(g) 10.65	10.44	(g) 18.27	18.73	(g) 17.88	18.51
			(dpi) 11.01	10.64				
			(11.21 ± 0.09)[d]					

[a] For the *a*IP's, results are given for adiabatic ionization into the anti (a), gauche (g), and disproportionated ion (dpi) of the ionization product. Results are given for calculations at the LSD level, and with exchange-correlation gradient corrections (GGC). Experimental values are given in parenthesis. Energies in units of electronvolts. [b] Reference 45. [c] Reference 26. [d] Reference 25.

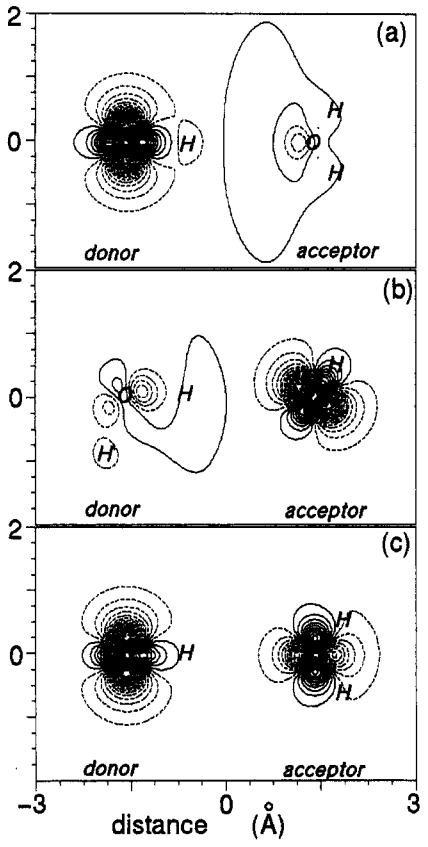

Figure 3. Contours of electron density differences for the following processes (dashed contours corresponding to a deficit of the electron density): (a) $\rho\{[(H_2O)_2]^+\} - \rho\{(H_2O)_2\}$, corresponding to the vertical first ionization of the neutral dimer resulting in the $^2A''$ state of the cation, plotted in the plane normal to that of the donor water molecule in the neutral dimer (see Figure 1), illustrating that the hole in $[(H_2O)_2]^+$ is predominantly localized on the donor molecule; (b) same as in (a) but for the second ionization of $(H_2O)_2$, resulting in the $^2A'$ state of the singly charged cation, plotted in the plane of the donor molecule (which contains the HOH bisector of the acceptor), illustrating that for the second ionization the hole is created mostly on the acceptor molecule; (c) $\rho\{[(H_2O)_2]^{2+}\} - \rho\{(H_2O)_2\}$, corresponding to direct vertical double ionization of the neutral dimer, plotted in the plane normal to that of the donor molecule of the neutral, illustrating two ionization holes, one on the donor and one on the acceptor molecule.

barrierless "autoprotonation" process, induced by the charge imbalance due to the localized ionization hole on the proton donor, involving a significant contraction of the interoxygen distance, and resulting in a stable disproportionated ion (dpi), $(OH)(H_3O^+)$, where $d_{O_1O_2} = 2.502$ Å, compared to 2.957 Å in $(H_2O)_2$ (see Figure 1 and Table 1). The relaxation energy gained in this process, which involves a large configurational change, is 1 eV, and thus the adiabatic ionization potential of the neutral dimer into the dpi state is $a\text{IP}[(H_2O)_2;+\text{dpi}] = 10.64$ eV. This should be compared to the aIP of the water molecule (calculated as 12.59 eV compared to an experimental value[25] of 12.6 eV), where the configurational relaxation upon ionization is minimal.

However, our calculations show that the $(OH)(H_3O)^+$ dpi state is not, as commonly believed,[26-28,30-32] the lowest energy isomer of the ionized dimer. Rather, we found that the optimal ground-state configuration of the dimer cation, which we denote as $(H_2O)_2^+$(a), is structurally hydrazine-like with $d_{O_1O_2} = 2.176$ Å (Figure 1 and Table 1). In this "anti" configuration the bisectors of the HOH angle of the two water molecules are oriented antiparallel to each other, and the ionization hole is delocalized. The $(H_2O)_2^+$(a) ground-state is lower in energy than the dpi isomer by 0.22 eV (i.e., $a\text{IP}[(H_2O)_2;+\text{a}] = 10.42$ eV) and the transformation of the vertically ionized dimer into the anti state most likely involves a barrier. In addition to the $(H_2O)_2^+$ (a) ground state, a slightly higher in energy (0.02 eV) isomer was found with the two water molecules of the dimer cation in a "gauche" relative orientation (denoted as $(H_2O)_2^+$(g); see Figure 1 and Table 1). We note here that all the above states of the dimer cation (the newly found anti and gauche configurations, and the dpi isomer) involve significant rearrangement of the electron distribution and nuclear positions with respect to that of the neutral dimer, driven by the ejection of an electron from a nonbonding type orbital of the neutral dimer. This results, as noted previously[28], in a small Franck–Condon factor between the minima of the hypersurfaces of the parent neutral and ionized dimer, which implies that the experimental threshold ionization energy does not coincide with the true adiabatic ionization energy.

Dissociation of the water dimer may occur via alternative channels:[26] (i) the "oxonium channel" (O), $(H_2O)_2 + h\nu \rightarrow H_3O^+ + OH + e^-$, and (ii) the "water channel" (W), $(H_2O)_2 + h\nu \rightarrow H_2O^+ + H_2O + e^-$. The calculated dissociation energies corresponding to these channels are (see Table 3): $E_d(O) = 11.67$ eV (compared to 11.73 eV determined from the photoion yield curve[25]), and $E_d(W) = 12.75$ eV (compared to the experimentally estimated value of 12.86 eV[28]). From Figure 2 we note that while the vertically ionized state, $[(H_2O)_2]^+$, may dissociate spontaneously into the O channel, its dissociation into the W channel requires an energy of 1.01 eV.

If the vertically ionized dimer relaxes into the OH $(H_3O)^+$ dpi isomer, dissociation into the O channel requires an energy of 1.02 eV (compared to an experimentally estimated[25] lower bound of 0.6 eV), and dissociation into the W channel requires 2.11 eV (compared to an experimental[25] lower bound of 1.6–1.7 eV). On the other hand, the vertically ionized dimer may relax into the $(H_2O)_2^+$(a), ground-state, or the $(H_2O)_2^+$(g) isomer, in a process entailing a large configurational change and involving a barrier, or conversion between the dpi and the a or g isomers may occur, involving a barrier of ~0.2 eV (the barrier for the reverse transformation is ~0.42 eV); indeed BO-

TABLE 3: Dissociation Energies for the Neutral Dimer $(H_2O)_2$, the $(H_2O)_2^-$(a), and $(OH)(H_3O)^+$ States of the Singly Charged Dimer Cation, the "Anti" Metastable Bound State of the Doubly Ionized Dimer, $(H_2O)_2^{2+}$(a), and for the Vertically Doubly Ionized Dimer in the Disproportionated-Ion Configuration, $[(OH)(H_3O)^+]^{+a}$

	$(H_2O)_2$		$(H_2O)_2^+$(a)		$(OH)(H_3O)^+$		$(H_2O)_2^{2+}$(a)		$[(OH)(H_3O)^+]^+$	
	LSD	GGC	LSD	GGC	LSD	GGC	LSD	GGC	LSD	GGC
O	12.34	11.67 (11.73)[b]	1.72	1.25	1.33	1.02 (0.6)[b]	−3.15 [2.28]	−4.32 [1.46]	−5.40	−5.67
W	13.50	12.75 (12.86)[c]	2.88	2.34	2.49	2.11 (1.6−1.7)[c]	−2.38 [1.60]	−3.81 [0.68]	−4.62	−5.17

[a] Results are given for the "oxonium" (O) and "water" (W) channels. Experimental results are given in parentheses, and barriers in brackets. Results are given from calculations at the LSD level and with exchange-correlation gradient corrections (GGC). Energies in units of electronvolts. [b] Reference 25. [c] Reference 28.

LSD-MD simulations of the (OH) H_3O^+ isomer thermalized at 150, 300, and 600 K, have shown that at the higher temperature, following several back-and-forth proton transfer events, a vibrationally excited $(H_2O)_2^+$(a) state was formed. Dissociation of the (a) state into the W and O channels requires dissociation energies of 2.34 and 1.25 eV, respectively. From the above we conclude that the O channel is energetically favorable and will dominate for cold parent dimers and low (near threshold) ionization energies. However, dissociation into the W channel may occur for higher excitation energies.

(b) Doubly Charged Cations. As aforementioned, vertical direct double ionization (ddi) of $(H_2O)_2$ (i.e., simultaneous removal of two electrons) requires an energy vIP(ddi) = 30.15 eV (the difference in the ionization energies into the spin S = 0 and S = 1 states of the vertically doubly ionized $[(H_2O)_2]^{2+}$ was found to be 0.01 eV). The vertically doubly ionized state may fission into $2H_2O^+$, i.e., the W channel for the doubly ionized dimer, with an energy gain $\Delta(W)$ = 4.8 eV, or along the corresponding O channel, i.e., $OH^+ + H_3O^+$, with a gain $\Delta(O)$ = 5.31 eV.

However, we found that the vertically doubly ionized $(H_2O)_2^{2+}$ ion, which is isoelectronic with hydrazine, $(NH_2)_2$, may relax into anti and gauche metastable bound isomers (of conformations similar to those shown in Figure 1, with different distances and angles, see Table 1), with a relaxation energy of 1.00 eV for both isomers; consequently the aIP for the ddi process of $(H_2O)_2$ into these states is 29.15 eV (we note here that for $(H_2O)_2^{2+}$ the (a) and (g) isomers are essentially degenerate while for $(NH)_2$ the (g) state is more stable by ~0.08 eV).

While the O dissociation channel (yielding $OH^+ + H_3O^+$) is energetically favorable, the direct double-ionization generates ionization holes on the two hydrogen-bonded water molecules leading to fission into $2H_2O^+$ (i.e., the W channel). BO-LSD-MD simulations of this process, starting from a low-temperature vertically ddi state, show that 88% of the released energy converts into translational kinetic energy of the separating H_2O^+ fragments and the rest coverts into rotational (6%) and internal vibrational (2%) energies of the H_2O^+ fragment originating from the donor molecule of the initial dimer, and mainly internal vibrational energy (~4%) of the other fragment (see Figure 4).

An alternative route to generate the doubly ionized $(H_2O)_2^{2+}$ ion is via sequential double ionization (sdi), where the second ionization follows (with a time delay) the first one. The vertical and adiabatic ionization energies of the (a) and (g) state of $(H_2O)_2^-$ are vIP[$(H_2O)_2^+$;a] = 20.24 eV and aIP[$(H_2O)_2^+$;a] = 18.74 eV (i.e., a relaxation energy of 1.5 eV; see Figure 2). While the energy gain in fission of the anti isomer, $(H_2O)_2^{2+}$-(a), into the O channel (yielding $OH^+ + H_3O^+$) is 4.31 eV and that into the W channel (yielding $2H_2O^+$) is smaller by 0.5 eV (i.e., 3.81 eV), dissociation is likely to occur into the later, energetically less favorable, channel, since this process involves a barrier of 0.68 eV, compared to a dissociation barrier of 1.46 eV for the O channel. Indeed, this is what we found in dynamical simulations, starting from ionization of $(H_2O)_2^+$ in the anti configuration.

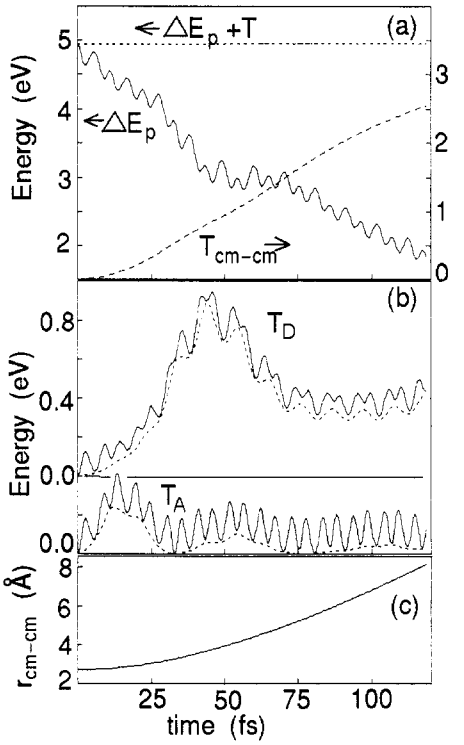

Figure 4. Results from an BO-LSD-MD simulation of the fission of the directly vertically doubly-ionized water dimer into the "water channel", $[(H_2O)_2]^{2+} \rightarrow H_2O^+ + H_2O^+$, starting from a very cold (~0 K) vertically doubly ionized water dimer. (a) The time evolution of the potential energy, ΔE_p (with reference to the potential energy of the products at infinite separation), and the translational kinetic energy of the center of mass separation, T_{cm-cm}. The dashed line, $\Delta E_p + T$, shows conservation of energy in the simulations. (b) Time evolution of the total internal kinetic energies (solid lines) of the fragments originating from the donor (T_D) and acceptor (T_A) molecules of the parent neutral, and corresponding rotational energies (dashed lines). In each case the internal vibrational energy is the difference between the solid and dashed lines. (c) Time evolution of the distance between the centers-of-mass of the fission fragments. Energies in electronvolts; time in femtoseconds.

However, the O channel may be observed when the second ionization in the sdi process starts from the dpi $(H_3O^+)OH$ isomer of the singly charged water dimer, with a vIP[(H_3O^+)-OH] = 19.87 eV when the resulting doubly ionized [(H_3O^+)-OH]$^+$ ion is in the spin S = 1 state and 20.28 eV when the latter is in the S = 0 state. The energy gain in fission of the disproportiate doubly ionized $[(H_3O^+)OH]^+$ intermediate (S = 1) into the O channel is 5.67 eV and that into the W one is 5.17 eV. While the $[(H_3O^+)OH]^+$ intermediate could transform into the more stable (a) or (g) isomers of the doubly charged dimer (with an energy gain of 1.36 eV), this relaxation involves

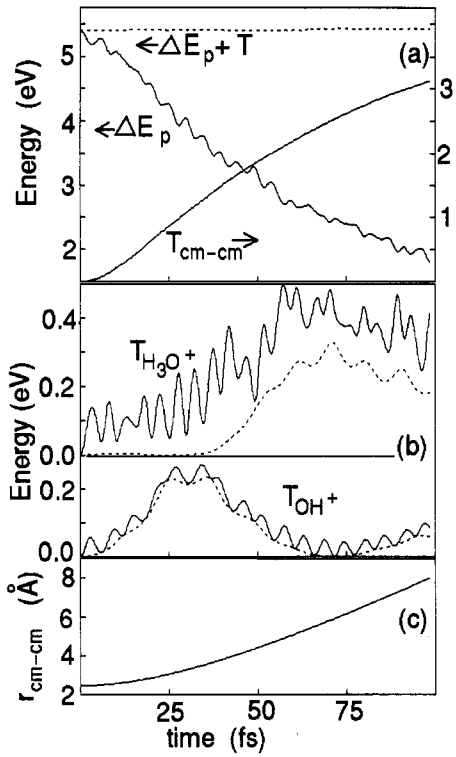

Figure 5. Same as Figure 4, but for the fission process of the vertically ionized disproportionated ion, resulting in fission into the "oxonium channel", $[(OH)(H_3O^+)]^+ \rightarrow OH^+ + H_3O^+$, starting from a cold ionized parent. Note that the H_3O^+ fragment is vibrationally hotter than the OH^+ fragment.

a significant structural rearrangement and is accompanied by a barrier. Consequently, fission into $OH^+ + H_3O^+$ occurs, as simulated by us starting from a cold $[OH(H_3O)^+]^+$ intermediate, with 92% of the released energy converted into interfragment translational energy, 4% and 2% into rotational and vibrational energies of H_3O^+, and the remaining 2% equally partitioned between the rotations and vibrations of OH^+ (see Figure 5).

4. Summary

We investigated, using accurate electronic structure calculations and molecular dynamics simulations, the energetics, structure, dynamics, ionization processes, and dissociation pathways of neutral and charged water dimer molecules. Our results for ionization potentials and dissociation energies agree with experimentally measured values (when available) and demonstrate that for these systems the inclusion of exchange-correlation gradient corrections improves the accuracy of the predicted values in a significant manner. Our main findings include the following:

(i) The ground-state of the singly charged cation, $(H_2O)_2^+$-(a), is in a hydrazine-like configuration, whose energy is predicted to be 0.22 eV below the disproportionated ion OH-$(H_3O)^+$ isomer (see Figure 1 and Table 1).

(ii) For cold neutral $(H_2O)_2$ and near threshold ionization, the dominant dissociation channel of the singly-charged dimer is into the oxonium (O) channel, $OH + H_3O^+$, with the water channel (W) (i.e., $H_2O + H_2O^+$) occurring for hotter parent dimers and larger excitation energies.

(iii) The doubly charged water dimer possesses a bound metastable $(H_2O)_2^{2+}$(a) state, which is nearly degenerate with a gauche isomer, and its dissociation into $2H_2O^+$ involves a barrier of ~0.68 eV.

(iv) The dissociation pathways of the doubly charged water dimer may depend on the ionization process. Direct vertical double ionization of the neutral ($vIP[(H_2O)_2;2+] = 30.15$) results in fission into the W channel, $H_2O^+ + H_2O^+$, while a sequential double ionization may lead to fission into the O channel, $OH^+ + H_3O^+$. Energetics and barriers for various dissociation pathways have been calculated (see Figure 2 and Table 3).

(v) BO-LSD-MD simulations of dissociation processes of the doubly ionized dimer show that ~90% of the released energy converts into translational kinetic energies of the fragments, and the rest is partitioned between rotations and vibrations of the fragments.

Acknowledgment. Research supported by the U.S. DOE (Grant No. DE-FG05-86ER-4234). Computations were performed on Cray computers at the National Energy Research Supercomputer Center at Livermore and the Georgia Institute of Technology Center for Computational Materials Science.

References and Notes

(1) *Intermolecular Forces*; Huyskens, P. L., Luck, W. A., Zeegers-Huyskens, T., Eds.; Springer: Berlin, 1991.
(2) *The Hydrogen Bond*; Schuster, P., Zundel, G., Sandorfy, C., Eds.; North-Holland: Amsterdam, 1976; Vols. 1–3.
(3) Arijs, E.; Nevejans, D.; Ingels, J.; Frederick, P. *J. Geophys. Res.* **1985**, *90*, 5891.
(4) Viggiano, A. A.; Dale, F.; Paulson, J. F. *J. Chem. Phys.* **1988**, *88*, 2469.
(5) Ferguson, E. E. *NATO Adv. Study Inst. Ser., Ser. B* **1979**, *VB40*, 377.
(6) Narcist, R. S.; Barley, A. D. *J. Geophys. Res.* **1965**, *70*, 3687.
(7) Fehsenfeld, F. C.; Dotan, I.; Albritton, D. L.; Howard, C. J.; Ferguson, E. E. *J. Geophys. Res.* **1978**, *90*, 1333.
(8) Arnold, F.; Krankowsky, O.; Marien, K. M. *Nature* **1977**, *267*, 30.
(9) Heurtas, M. L.; Fontan, J. *Atmos. Environ.* **1982**, *16*, 2521.
(10) Murad, E.; Bochsler, P. *Nature* **1987**, *326*, 366.
(11) Knewstubb, P. F.; Sugden, T. M. *Proc. R. Soc. London* **1960**, *A255*, 520.
(12) Kebarle, P.; Godbole, E. W. *J. Chem. Phys.* **1963**, *39*, 1131.
(13) Frisch, M. J.; Del Bene, J. E.; Binkley, J. S.; Schaefer, H. F. III *J. Chem. Phys.* **1986**, *84*, 2279.
(14) Lee, E. P. F.; Dyke, J. M. *Mol. Phys.* **1991**, *73*, 375 and references to earlier studies cited therein.
(15) Xie, Y.; Remington, R. B.; Schaefer, H. F. III *J. Chem. Phys.* **1994**, *101*, 4878 and references therein.
(16) See reviews in: Saykally, R. J. *Science* **1988**, *239*, 157. Coe, J. V.; Saykally, R. J. In *Ion and Cluster Ion Spectroscopy and Structure*; Maier, J. P., Ed.; Elsevier: Amsterdam, 1989; p 131. Guteman, C. S.; Saykally, R. *J. Annu. Res. Phys. Chem.* **1984**, *35*, 387.
(17) Good, A.; Durden, D. A.; Kebarle, P. *J. Chem. Phys.* **1970**, *52*, 212, 222.
(18) Olovsson, I. *J. Chem. Phys.* **1968**, *49*, 1063.
(19) Sears, T. J.; Bunker, P. R.; Davies, P. B.; Johnson, S. A.; Spirko, V. *J. Chem. Phys.* **1985**, *83*, 2676.
(20) Liu, D.-J.; Oka, T.; Sears, T. J. *J. Chem. Phys.* **1986**, *84*, 1312.
(21) Yeh, L. I.; Okumura, M.; Myers, J. D.; Price, J. M.; Lee, Y. T. *J. Chem. Phys.* **1989**, *91*, 7320.
(22) Okumura, M.; Yeh, L. I.; Myers, J. D.; Lee, Y. T. *J. Phys. Chem.* **1990**, *94*, 3416. Yeh, Y. I.; Lee, Y. T.; Hougen, J. T. *J. Mol. Spectrosc.* **1994**, *164*, 473.
(23) Shi, Z.; Ford, J. V.; Wei, S.; Castleman, A. W. Jr. *J. Chem. Phys.* **1993**, *99*, 8009.
(24) Wei, S.; Shi, Z.; Castleman, A. W. Jr. *J. Chem. Phys.* **1991**, *94*, 3266.
(25) Ng, C. Y.; Trevor, D. J.; Tiedemann, P. W.; Ceyer, S. T.; Kronebusch, P. L.; Mahan, B. H.; Lee, Y. T. *J. Chem. Phys.* **1977**, *67*, 4235.
(26) Tomoda, S.; Achiba, Y.; Kimura, K. *Chem. Phys. Lett.* **1982**, *187*, 197.
(27) Sato, K.; Tomoda, S.; Kimura, K.; Iwata, S. *Chem. Phys. Lett.* **1983**, *95*, 579.
(28) Tomoda, S.; Kimura, K. *Chem. Phys.* **1983**, *82*, 215.
(29) Moncrieff, D.; Hilliar, J. H.; Saunders, V. R. *Chem. Phys. Lett.* **1982**, *89*, 447.
(30) Curtiss, L. A. *Chem. Phys. Lett.* **1983**, *96*, 442.
(31) Shinohara, H.; Nishi, N.; Washida, N. *J. Chem. Phys.* **1986**, *86*, 5562.
(32) Stace, A. *J. Phys. Rev. Lett.* **1988**, *61*, 306; *Chem. Phys. Lett.* **1990**, *174*, 103.

(33) Haberland, H.; Langosch, H. *Z. Phys. D* **1986**, *2*, 243.
(34) Buck, U.; Winter, M. *Z. Phys. D* **1994**, *31*, 291.
(35) Barnett, R. N.; Landman, U. *Phys. Rev. B* **1993**, *48*, 2081.
(36) Barnett, R. N.; Landman, U. *Phys. Rev. Lett.* **1993**, *70*, 1775.
(37) Barnett, R. N.; Cheng, H.-P.; Hakkinen, H.; Landman, U. *J. Phys. Chem.* **1995**, *99*, 1995.
(38) Cheng, H.-P.; Barnett, R. N.; Landman, U. *Chem. Phys. Lett.* **1995**, *237*, 161.
(39) Laasonen, K.; Parrinello, M.; Car, R.; Lee, C.; Vanderbilt, D. *Chem. Phys. Lett.* **1993**, *207*, 208.
(40) Troullier, N.; Martins, J. L. *Phys. Rev. B* **1991**, *43*, 1993.
(41) (a) Becke, A. D. *Phys. Rev. A* **1988**, *38*, 3098. (b) Becke, A. D. *J. Chem. Phys.* **1992**, *96*, 2155.
(42) Perdew, J. P.; Wang, Y. *Phys. Rev. B* **1991**, *44*, 13298; **1991**, *43*, 8911; **1992**, *49*, 13244.
(43) Note that the value of 0.20 eV which we calculated in ref 35 (Table 2) was obtained from a post-LSD exchange-correlation correction.
(44) Curtiss, L. A.; Frurip, D. L.; Blander, M. J. *J. Chem. Phys.* **1979**, *71*, 2703.
(45) Kimura, K.; Katsumata, S.; Achiba, Y.; Yamazaki, T.; Iwata, S. *Handbook of HeI Photoelectron Spectra of Fundamental Organic Molecules*; Japan Scientific Societies Press/Halsted Press: Tokyo/New York, 1981; p 33.

JP952830I